Simultaneous Tracking of Multiple Targets using Interferometric FMCW Radar

Huaiyuan Liang[1], Pengcheng Wang[2], Xiangrong Wang[2*],
[1]Shenyuan Honors College, Beihang University, Beijing, China
[2]School of Electronic and Information Engineering, Beihang University, Beijing, China
[*]Email address: xrwang@buaa.edu.cn

This paper presents an approach for simultaneous tracking of multiple targets using the interferometric frequency modulated continuous wave (FMCW) radar. A dual-channel receiver FMCW radar is utilized for interferometric measurement. The trajectory of each target is estimated separately based on two-dimensional position and velocity, which can be extracted by applying stretch processing and time-frequency analysis to the interferometric echo signals simultaneously. The two-dimensional positions and velocities are input to a Kalman filter to improve tracking performance. Simulation and experimental results of walking people are presented to validate the performance of the approach.

***Index Terms*—Tracking, interferometric radar, stretch processing**

I. INTRODUCTION

Interferometric radar has the ability to take measurement of the angular velocity in tangential direction apart from the radial velocity, enabling target tracking in the case of known initial position [1]. For a continuous wave (CW) radar, frequency shift of the echo signal from a single receiving channel compared with the transmit signal is only induced by the Doppler effect, where the radial velocity relative to the radar antenna can be extracted by performing short-time Fourier Transform (STFT) to the beat signal. Considering the placement of two receiving antennas, the angular velocity is acquired by interferometric processing. Whereas in the actual scene, we are unable to acquire the initial position of the target using CW radar, which limits the application of this approach.

FMCW radar can be utilized to solve the aforementioned problem which provides range information of the target. However, to acquire high resolution in radial velocity measurement, the baseline between two receiving antennas is normally much larger than the wavelength corresponding to the operating frequency. In this case, conventional algorithms for direction-of-arrival (DOA) estimation in array processing induce strong angle ambiguity problem, making it difficult to determine the azimuth angle of the target. For linear frequency modulated waveforms, stretch processing is a more feasible method for angle measurement, which only requires the range information corresponding to two receiving channels.

In this paper, we propose a new approach for multiple target tracking using interferometric FMCW radar. The radial velocity and angular velocity of each target are estimated by performing time-frequency analysis to the beat signal. By applying stretch processing in combination with far field conditions, we are able to estimate the range and azimuth angle of the targets simultaneously. Considering two-dimensional position and velocity, the trajectories of the targets are able to be estimated with a relatively high precision.

This work is supported by National Natural Science Foundation of China under Grant No. 61701016.

II. INTERFEROMETRIC RADAR MEASUREMENTS

A. Interferometric FMCW Radar System

The radar system consist of one transmitting antenna and two receiving antennas spacing with a baseline D, which is illustrated in Fig. 1. In the radar processor, the received signals from two channels pass through a low noise amplifier (LNA) cascaded with a band pass filter (BPF), and then mixed with the transmit signal to get the beat signals, which are sampled for further degital signal processing.

B. Position Estimation

The position estimation is based on range and azimuth angle measurements. We assume that the radar transmits a linear frequency modulated signal with the carrier frequency f_0, bandwidth B, and sweep time T. In the same sweep period, the transmit signal can be expressed as,

$$s_T(t) = \exp\{j2\pi[f_0 t + \frac{K}{2}t^2]\}. \tag{1}$$

where $K = B/T$ is the chirp rate. Consider a target in the far field, whose range is R_1 relative to receive antenna 1 and R_2 relative to receive antenna 2. The time delay of the echo signal is,

$$\begin{aligned} \tau_1 &= 2R_1/c \\ \tau_2 &= 2R_2/c \end{aligned} \tag{2}$$

where c is the speed of the signal. As the Doppler shift is relatively small comparing with the frequency shift induced by the time delay, the target is assumed to be stationary during each sweep, and τ_1 and τ_2 are considered time-invariant. The received signals from two receive channels are described by,

$$\begin{aligned} s_{R1}(t) &= \exp\{j2\pi[f_0(t-\tau_1) + \frac{K}{2}(t-\tau_1)^2]\} \\ s_{R2}(t) &= \exp\{j2\pi[f_0(t-\tau_2) + \frac{K}{2}(t-\tau_2)^2]\} \end{aligned} \tag{3}$$

978-1-7281-2345-5/19/$31.00

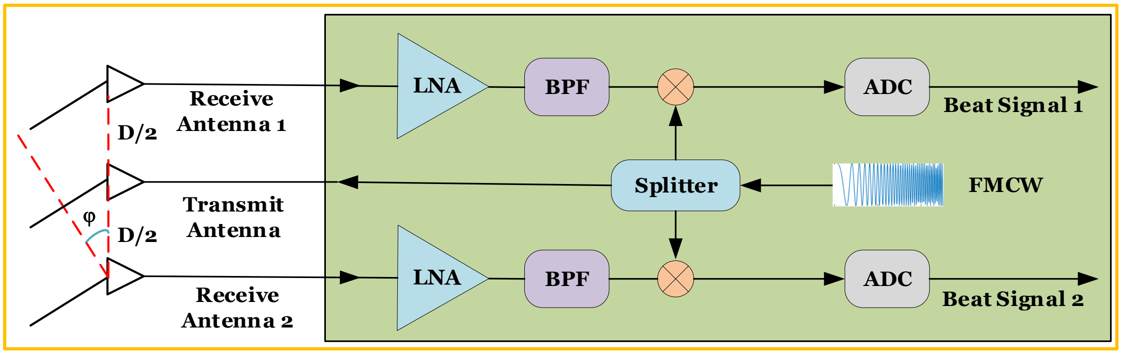

Fig. 1. Interferometric FMCW radar system diagram.

To apply stretch processing, the received signals are mixed with the transmit signal to form the beat signals.

$$\begin{aligned} s_{B1}(t) &= s_T(t) \otimes s_{R1}(t) \\ &= \exp\{j2\pi[f_0\tau_1 + \frac{K}{2}(2\tau_1 t - \tau_1^2)]\} \end{aligned} \tag{4}$$

$$\begin{aligned} s_{B2}(t) &= s_T(t) \otimes s_{R2}(t) \\ &= \exp\{j2\pi[f_0\tau_2 + \frac{K}{2}(2\tau_2 t - \tau_2^2)]\} \end{aligned} \tag{5}$$

The instantaneous frequency of the beat signal is the time derivitive of the phase term.

$$\begin{aligned} f_1 &= \frac{d}{dt}2\pi[f_0\tau_1 + \frac{K}{2}(2\tau_1 t - \tau_1^2)] \\ &= 2\pi K\tau_1 \end{aligned} \tag{6}$$

$$\begin{aligned} f_2 &= \frac{d}{dt}2\pi[f_0\tau_2 + \frac{K}{2}(2\tau_2 t - \tau_2^2)] \\ &= 2\pi K\tau_2 \end{aligned} \tag{7}$$

The time delay τ_1, τ_2 are obtained by performing FFT to the beat signals, where we can extract the range information of the target. The estimated range $\hat{R}_1$ and $\hat{R}_2$ are given by,

$$\hat{R}_1 = \tau_1 c/2 = \frac{cf_1}{4\pi K} \tag{8}$$

$$\hat{R}_2 = \tau_2 c/2 = \frac{cf_2}{4\pi K} \tag{9}$$

Although each one of the aforementioned range estimation can represent the range of the target, averaging the two estimation provides a more accurate result, in which case the midpoint of two receive antennas is taken as the reference position.

$$\hat{R} = \frac{\hat{R}_1 + \hat{R}_2}{2} \tag{10}$$

For a target in the far field, the echo can be considered as parallel wave. Hence the ranges referenced by two receiving antennas, the angle of arrival, and receiver baseline satisfy a specific geometric relationship, by which we can solve for the angle of arrival by,

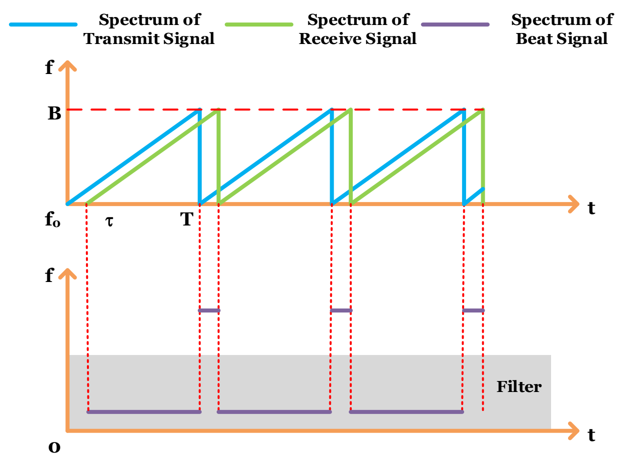

Fig. 2. The spectra of transmit, receive, and beat signal.

$$\hat{\varphi} = arcsin\frac{\hat{R}_1 - \hat{R}_2}{D} \tag{11}$$

where $\hat{\varphi}$ denotes the angle of arrival estimation and ranges from $-\pi/2$ to $\pi/2$.

Note that in the range measurement process, the fast-time sampling rate f_{sf} is far lower than the bandwidth of the transmit signal. If the beat signal passes through an anti-aliasing filter before sampling, the signal generated by transmit and receive signals in different sweep period will not be sampled, which is illustrated in Fig. 2. This allows us to sample for multiple sweep periods and process the sampling series by one FFT procedure, which increases the resolution of range and azimuth angle.

C. Velocity Estimation

In this section, we take the velocity of the target into consideration. Consider the range $\tilde{R}_1$ and $\tilde{R}_2$ as a function of time. Different from CW radar, since the Doppler frequency is combined with the frequency induced by the range of the target, the slow-time sampling rate f_{ss} for FMCW radar is restricted to be integer times of the sweep frequency. In order to achieve a high slow-time sampling rate, the sagnal is down-sampled to one sampling point for per sweep, therefore the slow-time sampling period $T_{ss} = T$.

Now we can eliminate the influence of frequency modulation, and the down-sampled beat signals can be expressed as,

$$\begin{aligned}\tilde{s}_{B1}(nT) &= \exp[j2\pi f_0 \tilde{\tau}_1(nT)] \\ &= \exp[j4\pi \tilde{R}_1(nT)/\lambda]\end{aligned} \tag{12}$$

$$\begin{aligned}\tilde{s}_{B2}(nT) &= \exp[j2\pi f_0 \tilde{\tau}_2(nT)] \\ &= \exp[j4\pi \tilde{R}_2(nT)/\lambda]\end{aligned} \tag{13}$$

where $\lambda = c/f_0$ is the wavelength, nT denotes the sampling instant in the nth sweep period, and time delays $\tilde{\tau}_1(nT)$, $\tilde{\tau}_2(nT)$, ranges $\tilde{R}_1(nT)$, $\tilde{R}_2(nT)$ changes with time. The Doppler frequency is the time derivitive of the phase term, which is,

$$\tilde{f}_1 = \frac{d}{dnT}[2\tilde{R}_1(nT)/\lambda] \qquad = 2\tilde{v}_1(nT)/\lambda \tag{14}$$

$$\tilde{f}_2 = \frac{d}{dnT}[2\tilde{R}_2(nT)/\lambda] \qquad = 2\tilde{v}_2(nT)/\lambda \tag{15}$$

where $\tilde{v}_1(nT)$ and $\tilde{v}_2(nT)$ are the radial velocities referring to the two revceive antennas. Hence by applying STFT to the slow-time data, we can get the time-Doppler map and extract the Doppler frequency, by which we can make an estimation of the radial velocity of the target $\hat{v}_1(nT)$ and $\hat{v}_2(nT)$. Similar to the range estimaiton, to achieve higher accuracy, the final estimation of the radial velovity is made using the average of $\tilde{v}_1(nT)$ and $\tilde{v}_2(nT)$, which is,

$$\hat{v}_r = \frac{\hat{R}_1 + \hat{R}_2}{2} \tag{16}$$

The angular velocity estimation also requires interferometry measurement. Consider the aforementioned geometric relationship in the far field,

$$\tilde{R}_1(nT) - \tilde{R}_2(nT) = D \sin\tilde{\varphi}(nT) \tag{17}$$

where the ranges $\tilde{R}_1(nT)$, $\tilde{R}_2(nT)$, and azimuth angle $\tilde{\varphi}$ are all time-varying. Take the time derivative of Eq. 18, we have the relationship between radial velocities and angular velocities.

$$\tilde{v}_1(nT) - \tilde{v}_2(nT) = D\cos\tilde{\varphi}(nT)\tilde{\omega}(nT) \tag{18}$$

where $\tilde{\omega}(nT)$ is the angular velocity at $t = nT$. Since we have the measurement of two radial velocities and azimuth angle, we are able to estimate the radial velocity by,

$$\hat{\omega}(nT) = \frac{\hat{v}_1(nT) - \hat{v}_2(nT)}{D\cos\hat{\varphi}(nT)} \tag{19}$$

D. Tracking Algorithm

Kalman filter is utilized to make an optimal estimation of the target trajectory fusing the two-dimensional position and velocity measurements. The state of the target at time instant k in polar coordinates can be expressed as,

$$\mathbf{x}_k = (\varphi, R, \omega, v_r)^T \tag{20}$$

which satisfies $\omega = \varphi'$ and $v_r = R'$. An estimate of the state is denoted as $\bar{\mathbf{x}}_k = (\bar{\varphi}, \bar{R}, \bar{\omega}, \bar{v_r})^T$. Since there is no known control input, the state at current instant can be expressed as,

$$\mathbf{x}_k = \mathbf{F}\mathbf{x}_{k-1} + \mathbf{v} \tag{21}$$

where $\mathbf{F}$ is the state transition matrix defined as,

$$\mathbf{F} = \begin{bmatrix} 1 & 0 & t & 0 \\ 0 & 1 & 0 & t \\ 0 & 0 & 1 & 0 \\ 0 & 0 & 0 & 1 \end{bmatrix} \tag{22}$$

And $\mathbf{v}$ is the process noise with covariance $\mathbf{Q}$. In the continuous white noise acceleration motion model [6], the covariance $\mathbf{Q}$ obeys,

$$\mathbf{Q} = \begin{bmatrix} \frac{1}{3}t^3 & 0 & \frac{1}{2}t^2 & 0 \\ 0 & \frac{1}{3}t^3 & 0 & \frac{1}{2}t^2 \\ \frac{1}{2}t^2 & 0 & t & 0 \\ 0 & \frac{1}{2}t^2 & 0 & t \end{bmatrix} q \tag{23}$$

where t is the time interval between consecutive measurements, and the process noise q is determined by the motion feature of the target.

An estimation of the state is predicted by the previous state,

$$\bar{\mathbf{x}}_{k|k-1} = \mathbf{F}\bar{\mathbf{x}}_{k-1} \tag{24}$$

and the predict error covariance is given by,

$$\mathbf{P}_{k|k-1} = \mathbf{F}\mathbf{P}_{k-1}\mathbf{F}^T + \mathbf{Q} \tag{25}$$

where $\mathbf{P}_{k-1}$ is the estimate covariance.

The state is updated by the measurement via an observation matrix $\mathbf{H}$, which represents the angular velocity w and radial velocity v_r in this scenario, i.e.,

$$\mathbf{H} = \begin{pmatrix} 1 & 0 & 0 & 0 \\ 0 & 1 & 0 & 0 \\ 0 & 0 & 1 & 0 \\ 0 & 0 & 0 & 1 \end{pmatrix} \tag{26}$$

The optimal Kalman gain $\mathbf{K}_k$ is then,

$$\mathbf{K}_k = \mathbf{P}_{k|k-1}\mathbf{H}^T(\mathbf{H}\mathbf{P}_{k|k-1}\mathbf{H}^T + \mathbf{R})^{-1} \tag{27}$$

where $\mathbf{R}$ is the covariance of the observation noise.

Since fast-time data is used for the position estimation and slow-time data is used for velocity estimation, the measurements of position and velocity are assumed uncorrelated.

The updated state estimate $\bar{\mathbf{x}}_k$ is determined by,

$$\bar{\mathbf{x}}_k = \bar{\mathbf{x}}_{k|k-1} + \mathbf{K}_k(\mathbf{Z}_k - \mathbf{H}\hat{\mathbf{x}}_{k|k-1}) \tag{28}$$

where $\hat{\mathbf{Z}}_k = (\hat{\varphi}_k, \hat{R}_k, \hat{\omega}_k, \hat{v}_{rk})^T$ is the measurement at time step k. The estimate covariance $\mathbf{P}_k$ is then updated according to,

$$\mathbf{P}_k = (\mathbf{I} - \mathbf{K}_k\mathbf{H})\mathbf{P}_{k|k-1} \tag{29}$$

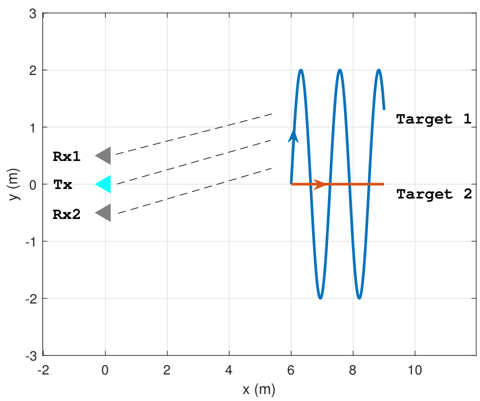

Fig. 3. The simulation setup diagram

III. Simulation Results

Simulation was made to validate the performance of the simultaneous tracking algorithm of multiple targets. Take the transmit antenna as reference, and assume it is located at $(0, 0)$. The receive antennas are distributed along the y axis on both sides of the transmit antenna, with a baseline $D = 1m$. Two targets are assumed to be an ideal points in the far field which moves along the trajectory described as

$$\begin{cases} x_1 = 6 + t & (m) \\ y_1 = 2\sin(5t) & (m) \end{cases} \tag{30}$$

and

$$\begin{cases} x_2 = 6 + t & (m) \\ y_2 = 0 & (m) \end{cases} \tag{31}$$

The antenna configuration and trajectories of the targets are illustrated in Fig. 3.

The radar operates at the frequency of $f_0 = 24GHz$ with a bandwidth $B = 2GHz$ and sweep time $T = 1ms$. The fast-time sampling rate $f_{sf} = 128kHz$ and the slow-time sampling rate $f_{ss} = 1/T = 1kHz$. White Gaussian noise was added to the signal and the SNR is $20dB$.

We can extract the fast-time and slow-time frequency shifts induced by two moving targets to measure the ranges and radial velocities of targets. The difference in radial velocities of two channels provides us with information about angular velocities. The estimated range, azimuth angle, radial velocity, and angular velocity of each target are processed by a Kalman filter, and Fig. 4 shows the processed measurements of the two targets. As is shown in the figure, the measurements of range, azimuth angle, and radial velocity performs good, while there is a distortion in the angular velocity measurement of target 1 when the angular velocity exceeds the maximum value.

The output of the Kalman filter gives the optimal estimation of the target trajectory presented in Fig. 5. The result indicates that the tracking approach is relatively accurate under our simulation conditions.

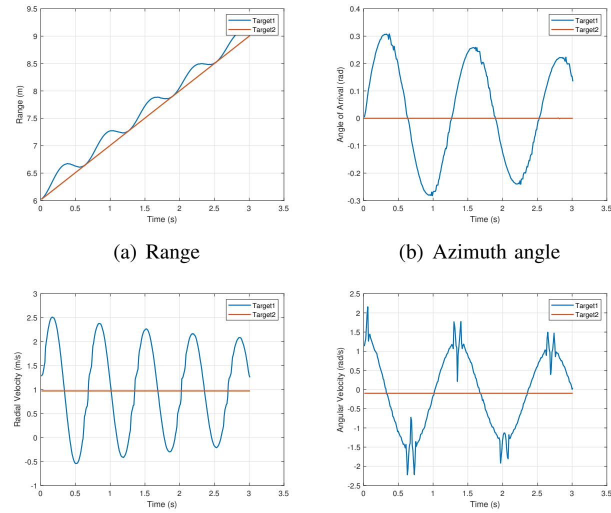

(a) Range (b) Azimuth angle (c) Radial velocity (d) Angular velocity

Fig. 4. The 2 dimensional position and velocity measurements of two targets

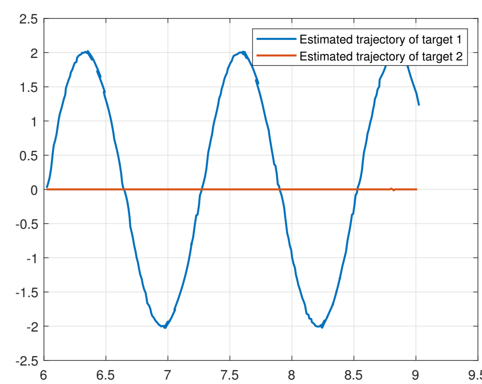

Fig. 5. The estimation of target trajectory after Kalman filtering

IV. Experimental Setup and Results

An Interferometric FMCW radar system is setup for the experiment. The system consists of one transmit antenna and two receive antennas, where the baseline of two receiving antennas is $D = 1$m. The radar transmits a 24GHz FMCW signal with a bandwidth of 750MHz and a sweeep time of 1ms. The sampling rate is set as 128kHz. Experiments have been carried out to validate the tracking performance for moving targets. The radar system is setup in the room and we take moving humans as targets, where the experimental scene is shown in Fig. 6. To satisfy the far field conition for interferometry, the distance between the antennas and human targets basically kept over 3 meters in the experiment, which is over three times longer than the baseline.

A. Scenario 1*: One Human Target Moving in Front of the Radar*

In this scenario, a human target moves in front of the radar. Both tracing in straight line back and forth and circling are

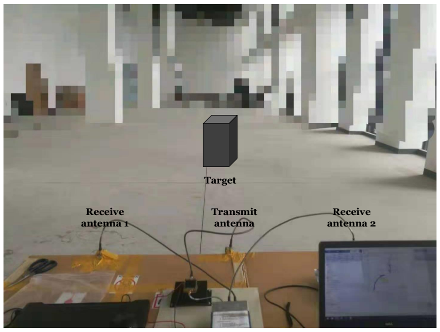

Fig. 6. The experimental scene of the radar system

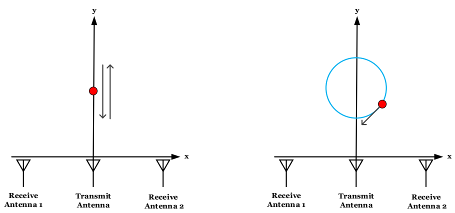

(a) Line (b) Circle

Fig. 7. The schematic diagram of one human target

tested in the experiment. The schematic diagram of scenario 1 is shown in Fig. 7.

Fig. 8 shows the original and Kalman filtered trajectory of the target by the Interferometric FMCW radar system. The instantaneous position of the target is extracted from the range and velocity information from two channels. Using interferometric measurement method, the angle of the target is very sensitive to the error of range, which induce unstable angular information. This causes that even we can get good estimation of the range of the target, but still the angular distance of the target between each frame is relatively long, which is shown by the scatters in Fig. 8. By Kalman filtering however, we are able to make a relatively good estimation of the trajectory which corresponds to the real track of the target, which shows the linear and circular traces of the monitored target.

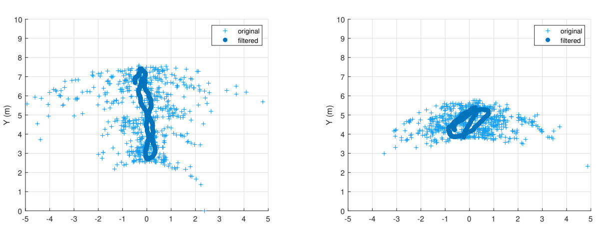

(a) Line (b) Circle

Fig. 8. The estimated trajectory of scenario 1

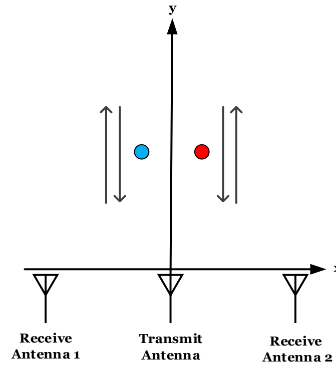

Fig. 9. The schematic diagram of two human target

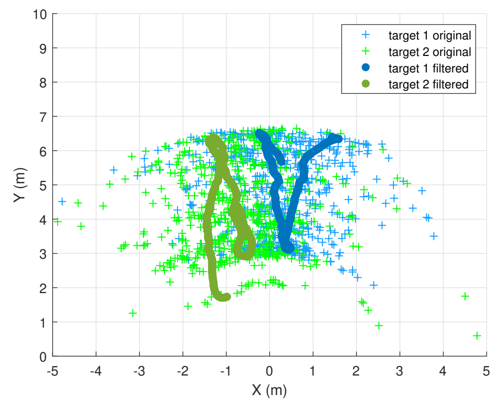

Fig. 10. The estimated trajectories of scenario 2

B. Scenario 2: Two Human Targets Moving in Front of the Radar

In this scenario, two human targets walk straightly in front of the radar, where the targets keep the opposite direction of moving at the same time. The schematic diagram of scenario 2 is shown in Fig. 9.

As there are two human targets moving simultaneously, we used nearest neighbor data association (NNDA) method to associate the range and velocity of each target. Then we pair the data from two channels by measuring the distance between the associated range sequences. The trajectory estimation algorithm is identical to the approach for single target. The trajectories of two targets are shown in Fig. 10. The experimental results match the true trajectories of the targets well.

V. Conclusion

In this paper, we proposed a tracking approach of multiple targets based on two-dimensional position and velocity measurement. The range and radial velocity are extracted using the fast-time and slow-time sampled signal. By performing interferometric measurements, the azimuth angle and angular velocity are estimated. The position and velocity information is processed by a Kalman filer to optimize the trajectory estimation. The simulation and experimental results indicate that the approach has good perform.ance in multiple targets tracking.

REFERENCES

[1] J. A. Nanzer, "Interferometric detection of the angular velocity of moving objects," 2010 IEEE MTT-S International Microwave Symposium, Anaheim, CA, USA, May 2010, pp. 1628-1631.

[2] J. A. Nanzer, "Resolution of interferometric angular velocity measurements," in Antennas and Propagation (APSURSI), 2011 IEEE International Symposium on, 2011, pp. 3229-3232.

[3] V. C. Chen, W. J. Miceli, "Time-varying spectral analysis for radar imaging of maneuvering targets," IEE Proceedings-Radar Sonar and Navigation, vol. 145, no. 5, pp. 262-268, 1998-Oct.

[4] E. J. Holder, "Angle-of-Arrival Estimation Using Radar Interferometry Methods and Applications," SciTech Publishing, Edison, NJ, 2014, pp. 148-151.

[5] J. R. Klauderer, A. C. Price, S. Darlington, and W. L. Albersheim, "The theory and design of chirp radars," Bell System Tech. J., vol. 39, 1996, pp. 745–808.

[6] R. B. Dybdal, "Monopulse resolution of interferometric ambiguities," IEEE Trans. AES, vol. AES-22, no. 2, pp. 177–183, 1986.

[7] E. J. Holder, "Angle-of-Arrival Estimation Using Radar Interferometry Methods and Applications," SciTech Publishing, Edison, NJ, 2014, pp. 162-165.

[8] Y. Lu, L. Huang, "Experimental Study on Moving Target Localization Using Dual Frequency Continuous Wave Radar," IEEE Radar Conf, Boston, MA, USA, April, 2019.

[9] X. Wang, H, Liang, P. Wang, "Detection and Tracking of UAVs using Interferometric Radar," SEE Radar 2019, Toulon, France, Sept. 2019 (accepted).

[10] M. Ritchie, F. Fioranelli, H. Griffths, and B. Torvik, "Micro-Drone RCS Analysis," Proc. of IEEE Radar Conference, Johannesburg, South Africa, Oct. 2015, pp. 452-456.

[11] Y. Bar-Shalom, X. Li, and T. Kirubarajan, "Estimation with Applications to Tracking and Navigation," 2001, pp. 269-272.